



Title	Brown carbon in atmospheric outflow from the Indo-Gangetic Plain: Mass absorption efficiency and temporal variability
Author(s)	Srinivas, Bikkina; Sarin, M. M.
Citation	Atmospheric Environment, 89, 835-843 https://doi.org/10.1016/j.atmosenv.2014.03.030
Issue Date	2014-06
Doc URL	http://hdl.handle.net/2115/56410
Type	article (author version)
File Information	AE 89_835-843.pdf



[Instructions for use](#)

**Brown carbon in atmospheric outflow from the Indo-Gangetic Plain:
Mass absorption efficiency and temporal variability**

By

Bikkina Srinivas and M. M. Sarin*

Physical Research Laboratory, Ahmedabad -380009, India

**Revision Submitted to
“*Atmospheric Environment*”
(09 March 2014)**

*** *Corresponding author:***

Dr. M. M. Sarin,
Senior Professor
Geosciences Division
Physical Research Laboratory
Tel: + 91 79 26314306
E-mail: sarin@prl.res.in

Abstract

The simultaneous measurements of brown carbon (BrC) and elemental carbon (EC) are made in ambient aerosols (PM_{2.5}), collected from a site in north-east India during November'09-March'10, representing the atmospheric outflow from the Indo-Gangetic Plain (IGP) to the Bay of Bengal (BoB). The absorption coefficient of BrC (b_{abs}), assessed from water-soluble organic carbon (WSOC) at 365 nm, varies from 2 to 21 Mm⁻¹ and exhibits significant linear relationship ($P < 0.05$) with WSOC concentration (3 – 29 µg m⁻³). The angstrom exponent (α : 8.3 ± 2.6 , where $b_{abs} \approx \lambda^{-\alpha}$) is consistent with that reported for humic-like substances (HULIS) from biomass burning emissions (BBE). The impact of BBE is also discernible from mass ratios of nss-K⁺/EC (0.2 – 1.4) and OC/EC (3.4 – 11.5). The mass fraction of WSOC (10 – 23 %) in PM_{2.5} and mass absorption efficiency of BrC ($\sigma_{abs-BrC}$: 0.5 – 1.2 m² g⁻¹) bring to focus the significance of brown carbon in atmospheric radiative forcing due to anthropogenic aerosols over the Indo-Gangetic Plain.

Words: 161

1. Introduction

The light absorbing species of atmospheric particulate matter are gaining considerable interest in recent years owing to their significant role in regional as well as global climate change [Fuzzi *et al.*, 2006]. Although several studies have evaluated their impact on the atmospheric environment, uncertainties associated with the regional scenario are still large and demand further detailed assessment. One of the possible sources of uncertainty could be attributed to poor characterization of organic aerosols in the atmospheric particulate matter [Huebert and Charlson, 2000]. In this context, detailed information on sources, size-distribution and compositional changes during transport of carbonaceous aerosols is essential for assessing their atmospheric radiative forcing.

Among the carbonaceous species, two distinct forms of carbon [elemental or black carbon (EC or BC) and brown carbon (BrC)] are of particular interest due to their light absorbing properties. The EC absorbs solar radiation in the visible region [Bond, 2001; Bond *et al.*, 2013], whereas BrC shows prominent absorption in the near UV-region [Alexander *et al.*, 2008; Andreae and Gelencsér, 2006; Hecobian *et al.*, 2010; Lack *et al.*, 2012; Liu *et al.*, 2014; Lukács *et al.*, 2007; Yang *et al.*, 2009]. However, real time data on absorption properties of BrC are rather limited. The omnipresence of BrC in rural, urban and remote environments has been emphasized by Graber and Rudich, [2006] suggesting the need for its adequate representation in climate model simulations.

The presence of brown carbon is documented based on the absorption spectra of aqueous extracts of ambient aerosols [Havers *et al.*, 1998; Kirchstetter *et al.*, 2004; Zhang *et al.*, 2013]. Furthermore, its abundance has been studied using aerosol light absorption measurements near to the specific combustion sources [Bond, 2001]. A significant overlap in the spectral properties of BrC (assessed from water-soluble organic carbon, WSOC) and humic-like substances (HULIS), derived from the biomass burning emissions, has been reported during the LBA-SMOCC (Large scale Biosphere atmosphere experiment in Amazonia – SMOke aerosols, Clouds, rainfall and Climate) Experiment [Hoffer *et al.*, 2006]. The emission from biomass burning is recognized as a primary source of HULIS and of brown carbon [Andreae and Gelencsér, 2006; Park *et al.*, 2010]. It has been also suggested that tar balls from smoldering combustion of bio-fuels (or biomass) are a significant source of atmospheric brown carbon [Chakrabarty *et al.*, 2010]. In addition to emissions from specific sources, formation of brown carbon through heterogeneous reactions of secondary organic aerosols (emitted from biogenic and anthropogenic precursors like terpenes) with ammonia is also documented by Updyke *et al.*, [2012].

Uncertainties in atmospheric radiative forcing estimates continue to cause major debate (IPCC-2007), largely arising from the poor representation of the organic carbon fraction in atmospheric aerosols [Forster, 2007]. More recently, Feng et al., [2013] have emphasized the importance of brown carbon absorption in aerosol radiative forcing ($\sim 0.25 \text{ W.m}^{-2}$) using a general circulation model coupled to a chemical transport model. Their results suggest that atmospheric brown carbon could contribute nearly 19 % of the total absorption by anthropogenic aerosols; whereas 71 % is attributable to that from BC (or EC) and ~ 9 % is from sulphates and coatings of non absorbing organic compounds on soot carbon [Feng et al., 2013]. Furthermore, their study also highlights an overall mismatch between observations and model results for the simulated aerosol radiative forcing and suggests the need to incorporate absorption due to brown carbon in the global models. In this study, we have made simultaneous measurements of BrC and EC in ambient aerosols ($\text{PM}_{2.5}$) collected from a downwind sampling site in the Indo-Gangetic Plain, representing the atmospheric outflow. We have also assessed the mass absorption efficiency of BrC from water-extracts of aerosols.

2. Materials and Methods

2.1. Site description and meteorology

The Indo-Gangetic Plain (IGP), situated in the northern part of the Indian peninsula, generates a host of airborne pollutants. Fossil-fuel combustion, biomass burning (mainly agricultural crop-residue) and bio-fuel (wood) are some of the characteristic sources of pollutants. The impact of anthropogenic aerosols on oceanic regions located downwind of pollution sources in the Indo-Gangetic Plain has been well documented through field experiments such as INDOEX (Ramanathan et al., 2001; Lelieveld et al, 2001; Mayol-Bracero et al., 2002) and ICARB (Sudheer and Sarin, 2008; Sarin et al., 2011; Kumar et al., 2008; Srinivas and Sarin, 2012; Srinivas and Sarin, 2013). Under favourable meteorological conditions (shallow boundary height and north-easterly/westerly winds), the downwind transport of pollutants from the IGP to the Bay of Bengal is a conspicuous feature during the wintertime (from December to March).

Ambient aerosols ($\text{PM}_{2.5} \approx$ particulate matter whose aerodynamic diameter is less than $2.5 \mu\text{m}$) were collected during November'09 - March'10 from a downwind site (Kharagpur: 22.3°N , 87.3°E) in the Indo-Gangetic Plain (IGP). During the wintertime, the sampling site is influenced by long-range transport of pollutants from upwind sources in the IGP. Surface level meteorological parameters were obtained from NCEP (National Centre for

Environmental Predictions)-NCAR reanalysis data sets. The winds were predominantly north-easterly (0.5 to 3.8 m s^{-1}), and relative humidity and surface temperature varied from 38 to 58 % and 21.5 to $30.4 \text{ }^{\circ}\text{C}$, respectively. The air mass back trajectories (7-day AMBTs), computed from the NOAA website using hybrid single particle Lagrangian integrated trajectory model (HYSPLIT, version 4.0; [Draxler, 2002]), suggest transport of pollutants from the upwind source regions.

2.2. Methodology

Aerosol samples ($\text{PM}_{2.5}$, $N = 46$) were collected on pre-combusted tisuquartz filters (PALLFLEX[®]TM) using a high-volume ($\sim 1.13 \text{ m}^3 \text{ min}^{-1}$) air sampler (HVS- $\text{PM}_{2.5}$, Thermo-Anderson Inc.,). Most of the samples ($N = 42$) were collected over a period of ~ 22 hrs. After collection, all samples were stored in a deep freezer at -19°C until the time of their chemical analysis. For all chemical analyses, sample filters were handled under a clean laminar flow bench (Class – 1000). The absorption spectra of aqueous extracts of aerosols were measured on a UV-Vis Spectrophotometer (Model: USB-4000) coupled to a 2 m long waveguide capillary column. Deuterium and tungsten halogen lamps (DT-Mini-2, Ocean Optics) are used as a light source. Liquid samples were injected via capillary injector into Liquid-core Waveguide Capillary Cell (LWCC from World Precision Instrument, Sarasota, FL), with an internal volume of $250 \text{ }\mu\text{L}$. Absorption spectra were recorded over a wavelength range of 300 to 800 nm with an Ocean Optics Spectra-Suite data acquisition software system (Ocean Optics, Dunedin, FL). Simultaneously, concentrations of organic and elemental carbon (OC and EC) were also measured by thermo-optical transmittance method using Sunset-Lab EC-OC Analyzer. Water-soluble organic carbon (WSOC) was measured on total organic carbon analyzer (model: Shimadzu, TOC-5000a). Along with the samples, filter (and field) blanks were also analyzed for OC and WSOC. The contribution from blank signals was found to vary from 4 to 29 % and 0.1 to 14 % of the maximum and minimum signals measured for OC and WSOC, respectively. Based on the repeat measurements, the overall analytical reproducibility was better than 5 % for OC and WSOC, whereas it was less than 10 % for EC. For further details regarding the experimental protocol and method detection limits for OC, EC and WSOC, reference is made to our earlier publications [Ram *et al.*, 2010; Rengarajan *et al.*, 2007].

2.3. Absorption coefficient

In this study, absorption spectra of water extracts of aerosols (representing bulk of the water-soluble organic carbon) have been used to assess the absorption coefficient (b_{abs}) similar to that described by Hecobian et al., [2010] and is expressed as:

$$b_{abs} = (A_{365} - A_{700}) \times (V_{ext} \times 8) \times \ln(10) / (V_{aero} \times L)$$

In this equation, A_{365} and A_{700} correspond to measured absorbance at 365 and 700 nm, respectively. V_{ext} refers to volume of the aqueous extract (~ 50 ml) in which 1/8th portion of aerosol filter is extracted and factor '8' is used to estimate the absorption signal for the full filter. V_{aero} corresponds to volume of air filtered (~ 1400 m³ = 1.4 x 10⁹ ml) through quartz substrates and L is the path length of the cell (i.e., ~ 2 m). We have used absorbance at 365 nm to estimate the absorption coefficient (b_{abs}) of light absorbing water-soluble organic carbon (also referred as BrC). It is relevant to state that light absorption by OC in solvent extracts is underestimated by a factor of two than that of particulate OC [Liu et al., 2013]. Earlier studies have investigated the association of brown carbon with humic like substances in ambient aerosols [Lukács et al., 2007 and references therein]; however, separation of these compounds from the aqueous filter extracts is rather complex and experimentally tedious. Based on the replicate analyses of samples (N = 15), reproducibility of the absorbance signal was ascertained to be within 5 %. The contribution from filter blank to sample signal varied from 0.13 to 1.5 % of the maximum and minimum signal measured on LWCC. The error propagation, involving sample collection, extraction and measurement of WSOC, yield an analytical uncertainty of no more than 19 % in the mass absorption efficiency of light absorbing WSOC.

3. Results and Discussion

3.1. Angstrom exponent (α) and Mass Absorption efficiency (MAE or σ_{abs})

The absorption coefficient of an aerosol in the ambient atmosphere is a function of wavelength of incident light, and is described by a power law. The power exponent of wavelength is referred as Angstrom exponent (α) of a particular species and its magnitude depends on aerosol size and composition. Using a similar analogy, Hecobian et al., [2010] have described absorption coefficient of a light absorbing species in the aqueous extracts which is dependent on wavelength, and is given by the following relation.

$$b_{abs} \sim \lambda^{-\alpha}$$

$$b_{abs} \approx K \cdot \lambda^{-\alpha} ; K = \text{constant}$$

Here b_{abs} is expressed in units of M m⁻¹ (or 10⁻⁶ m⁻¹) and α denotes Angstrom Exponent of light absorbing component of water-soluble organic matter, referred here as Brown Carbon

(BrC). A value of ~ 7 for α has been reported for humic like substances extracted from aerosols, sampled from the Amazonian forest fires [Hoffer *et al.*, 2006]. Likewise, smoke from smouldering of various bio-fuels has a typical value for α between 7 and 16 [Chen and Bond, 2010]. Likewise, in an earlier study by Bones *et al.*, [2010], have estimated α as ~ 7 for freshly formed secondary organic aerosols (SOAs) compared to that observed for aged SOAs (~ 4.7). More recently, Hecobian *et al.*, [2010] have reported that α ranges between ~ 6 and 8 for biomass burning aerosols. However, their study also indicates that significant differences are observed between the biomass burning and non-burning periods.

In this study, absorption spectra of aqueous extracts were recorded between 300 nm and 800 nm for each sample. The absorbance at 365 nm (in near UV region) relative to 700 nm was obtained for all samples in order to estimate b_{abs} . Earlier studies have documented strong UV-absorption of water-soluble BrC at 350 to 370 nm [Hecobian *et al.*, 2010 and references therein]. Therefore, we attribute the prominent absorption at this wavelength range to the presence of brown carbon (BrC), in order to estimate the absorption coefficient of water-soluble organic carbon ($b_{abs-365}$). It is noteworthy that a significant linear relationship (slope = 0.70; $R^2 = 0.54$; P-value < 0.05) is observed between ($b_{abs-365}$) and WSOC (Fig.1); validating dominant absorption due to BrC in the water-extracts. Furthermore, co-variability in the temporal trend between concentration of WSOC and non-sea-salt-potassium ion (nss- K^+), suggests their common source from biomass burning emissions (Fig.2a). A significant correlation between WSOC and OC (P-value < 0.05) with an average WSOC/OC ratio of 0.52 ± 0.10 has been reported during the study period [Srinivas and Sarin, 2013b]. It is, thus, inferred that BrC contribute significantly to the mass concentration of particulate organic carbon in the atmospheric outflow from the IGP.

Further, we have calculated b_{abs} at varying wavelength (from 300 to 700 nm) relative to 700 nm. The b_{abs} shows wavelength dependency as $\lambda^{-\alpha}$, where α refers to Angstrom exponent (see supporting figure, Fig. S1). It is evident that the absorption signal of WSOC shows a sharp increase with decrease in wavelength (i.e., $b_{abs} \sim \lambda^{-6}$; See Table S1 for goodness of fit parameters for the power relation) and, thus, confirming the presence of brown carbon in aqueous extracts. This is consistent with earlier observations demonstrating the similar spectral absorption characteristics of the ambient particulate matter [Andreae and Gelencsér, 2006; Cheng *et al.*, 2011; Hecobian *et al.*, 2010; Lukacs *et al.*, 2007]. The angstrom exponent (α) of light absorbing WSOC in the IGP-outflow varied from 4.5 to 9.9 (Av: 6.0 ± 1.1). However, for most of the sampling days, α values are greater than 6 (Fig.2b).

The impact of biomass burning emissions is also evident through other diagnostic ratios (high OC/EC: 7.0 ± 2.0 and nss-K⁺/EC: 0.49 ± 0.21) in the IGP-outflow [Srinivas and Sarin, 2013b]. As stated above, for HULIS type compounds from biomass burning emissions and bio-fuel emissions, the angstrom exponent is reported to be greater than 6. Recently, Cheng et al., [2011] have estimated \AA_p value of ~ 7 in the aqueous extracts of aerosols from the Beijing outflow and attributed it to the presence of Brown Carbon. Therefore, the major source of BrC over the Indo-Gangetic Plain is attributed to biomass and bio-fuel burning during the study period. A more recent study by Zhang et al., [2013] had demonstrated the significant differences in the angstrom exponent of light absorbing WSOC between the offline filter-based aqueous ($\sim 7.6 \pm 0.5$) and methanol ($\sim 4.8 \pm 0.5$) extracts with those obtained through online measurements using PILS ($\sim 3.2 \pm 1.2$). However, the angstrom exponent of light absorbing WSOC measured at 365 nm (this study) is consistent with that reported for biomass burning emissions (See Table 1).

We have also estimated the mass absorption efficiency of light absorbing water-soluble organics as follows.

$$\text{MAE of BrC} = \sigma_{\text{abs-BrC}} (m^2 g^{-1}) = (b_{\text{abs-365}})/\text{WSOC}$$

In this study, the $\sigma_{\text{abs-BrC}}$ varied between 0.21 and 1.46 (Av: 0.78 ± 0.24) $m^2 g^{-1}$ in the atmospheric outflow from Indo-Gangetic Plain (Fig.2b). The slope of regression line ($0.70 m^2 g^{-1}$) in Fig. 1 also provides a robust estimate of mass absorption efficiency of BrC ($\sigma_{\text{abs-BrC}}$) in the atmospheric outflow from the Indo-Gangetic Plain. Lack et al., (2012) have reported a $\sigma_{\text{abs-BrC}}$ of $0.83 \pm 0.42 m^2 g^{-1}$ (measured at 404 nm using multi-wavelength Photo Acoustic measurements), in aerosols collected from the intense biomass burning emissions. Likewise, Hecobian et al., (2010) had reported a $\sigma_{\text{abs-BrC}}$ of ~ 0.60 and $0.58 m^2 g^{-1}$ for urban and rural sites, respectively (those characterized by high concentrations of levoglucosan). It is noteworthy that the mass absorption efficiency of BrC ($\sigma_{\text{abs-BrC}}$) documented for the IGP-outflow is consistent with that for biomass burning emissions reported in the literature [Hoffer et al., 2006; Lack et al., 2012; Yang et al., 2009]; as summarized in Table 1.

3.2. Source apportionment

The light absorbing organics in the atmosphere can originate either from primary or secondary processes. Incomplete combustion of biomass/bio-fuel burning and smoldering combustion processes are suggested as significant primary sources of brown carbon [Chakrabarty et al., 2010; Chakrabarty et al., 2013; Cheng et al., 2011; Hecobian et al., 2010; Hoffer et al., 2006; Kirchstetter and Thatcher, 2012; Lukacs et al., 2007]. However,

recent studies have documented the possible formation of atmospheric brown carbon through secondary processes such as heterogeneous reactions of isoprene in the presence of sulphuric acid vapour [Limbeck *et al.*, 2003]. Also, through multiphase chemistry of lignin type of compounds in the cloud water [Gelencser *et al.*, 2003; Gelencser and Varga, 2005; Nguyen *et al.*, 2010; Nguyen *et al.*, 2012], low temperature combustion of lignin pyrolysis products [Sareen *et al.*, 2010] and reaction of secondary organic aerosols with NH_3 [Nguyen *et al.*, 2013; Updyke *et al.*, 2012]. Therefore, in order to assess the sources of atmospheric brown carbon, primary and secondary organic carbon fractions were estimated for the sampling days using EC-tracer method [Ram and Sarin, 2010; 2011].

A notable feature of the data is seen as co-variability in the temporal trends of both primary and secondary organic carbon fractions with WSOC (See Supporting Fig. S2). The fractional contribution of OC_{sec} in total organic carbon (OC) varied from 11 to 70 % (Av: 50 ± 15 %). Although analytical uncertainty is large in the assessment of secondary organic carbon (OC_{sec}) based on EC-tracer method, it can be inferred that OC_{sec} contributes significantly to the total OC in the IGP-outflow during November'09-March'10. It is noteworthy that the mass absorption coefficient of light absorbing WSOC ($b_{\text{abs-365}}$) shows a positive correlation with estimated abundance of secondary organic carbon (OC_{sec}) and nss-K^+ (Fig.3). As stated earlier, OC_{sec} can be sourced from the atmospheric reactions of precursor VOCs produced from either biomass burning emissions or from fossil-fuel combustion sources. A recent study by Zhang *et al.*, [2011] had shown significant differences in the light absorption properties of water-soluble organic carbon in aerosols derived from fossil-fuel combustion (wherein absorption signal measured at 365 nm is relatively 4 to 6 times higher) and that from biomass burning emissions collected over Los Angeles and Georgia, respectively. Furthermore, their study highlighted the enhancement in light absorption by secondary aerosols of nitro aromatics from fossil-fuel combustion sources over Los Angeles. In the IGP-outflow, temporal variability in the mass absorption efficiency of light absorbing WSOC (measured at 365 nm) is not significant during the study period (November'09- March'10) and is consistent with that reported for biomass burning emission (Table 1). Based on these observations, a likely explanation could be that biogenic secondary organic aerosols contribute significantly to light absorbing organics over the Indo-Gangetic Plain.

In a laboratory study, Nguyen *et al.*, [2013] have documented the formation of light absorbing organic species based on reaction of ketolimononaldehyde ($\text{C}_9\text{H}_{14}\text{O}_3$), a SOA formed by the ozonolysis of limonene ($\text{C}_{10}\text{H}_{16}$), with amino acids (e.g. glycine) and NH_4^+ . A

similar study by Saleh et al., [2013] had provided the first direct evidence for the formation of light absorbing organics through secondary processes in the aged biomass/bio-fuel burning aerosols. In this study, we have not investigated the atmospheric reactions of SOAs at the molecular level. Nevertheless, in view of significant linear relationship among OC_{sec} , mass absorption efficiency of WSOC ($\sigma_{abs-WSOC}$ at 365 nm) and $nss-K^+$ (a proxy for biomass burning emissions), it can be inferred that secondary aerosol formation contribute significantly to atmospheric brown carbon.

Long ago, it was suggested by Andr ea [1983] that the association of potassium with soot carbon (or EC) in ambient aerosols signifies the importance of biomass/bio-fuel burning emissions. Since then, the mass ratio of $nss-K^+/EC$ in fine mode aerosols has been used as a proxy for assessing the qualitative contribution of biomass burning emissions [Andreae et al., 1984; Andreae and Merlet, 2001; Flament et al., 2011; Guazzotti et al., 2003; Ram and Sarin, 2010; Srinivas et al., 2011; Wang et al., 2005]. It is noteworthy that the $nss-K^+/EC$ ratio in the IGP-outflow during November'09-March'10 (Figure 4) is consistent with that reported for biomass/bio-fuel burning emissions. Based on radiocarbon data, Gustaffson et al., [2009] highlighted the significance of residential bio-fuel and agricultural crop-residue burning emissions from the IGP as a major source of carbonaceous aerosols over the south Asia (particular in the Northern India). In addition, it has also been suggested that biomass burning emissions contribute significantly to atmospheric water-soluble (primary and secondary) organics [Kawamura et al., 2013; Sciare et al., 2008; Timonen et al., 2012]. However, the volatile organic compounds (VOCs) emitted from the biomass/bio-fuel burning also contribute to atmospheric water-soluble organics through photochemical aging during the long-range atmospheric transport. In this regard, several studies have documented the high WSOC/OC and OC_{sec}/OC ratios from the biomass burning emissions [Agarwal et al., 2010; Favez et al., 2009; Sciare et al., 2008].

As stated earlier, the study site is influenced by long-range transport of bio-mass/bio-fuel burning emissions from the upwind source regions in the IGP. We have investigated the temporal variability of WSOC/OC, $nss-K^+/EC$, $\sigma_{abs-BrC}$ and OC_{sec}/OC (Fig.4). No significant ($P > 0.05$) differences are observed for the diagnostic mass ratio of $nss-K^+/EC$ during the sampling period (See Table S2). A large spread in the $nss-K^+/EC$ ratio for biomass burning emissions has been reported [Mayol-Bracero et al., 2002; Novakov et al., 2000] compared to that for fossil-fuel combustion. The near constancy of monthly-mean $nss-K^+/EC$ ratio overlaps with the reported range for BBEs. It is also noteworthy that near constancy of mass

absorption efficiency of light absorbing WSOC ($\sigma_{\text{abs-WSOC}}$) is comparable with that documented for biomass burning emissions [Cheng *et al.*, 2011; Hecobian *et al.*, 2010; Kirillova *et al.*, 2014].

A near constancy of $\text{nss-K}^+/\text{EC}$ and mass absorption efficiency of light absorbing water-soluble carbon ($\sigma_{\text{abs-WSOC}}$) in the IGP-outflow to the Bay of Bengal (Supporting information, one-way ANOVA results given in Table S2) indicate biomass burning emissions as a significant source of brown carbon over the study site. Several studies have suggested that biomass burning emissions contribute significantly to atmospheric water-soluble organics [Falkovich *et al.*, 2005; Graham *et al.*, 2002; Mayol-Bracero *et al.*, 2002; Saarikoski *et al.*, 2007; Sciare *et al.*, 2008; Timonen *et al.*, 2012]. Although WSOC/OC ratio exhibits small variability during the winter months (December-February; $\text{Av} \pm \text{Sd}$: 0.50 ± 0.13 ; $P > 0.05$); lower (0.41 ± 0.04) and higher (0.70 ± 0.18) contribution of WSOC to total OC is noteworthy in early and late sampling days in November and March. The relatively high mass ratio of WSOC/OC in the early spring-intermonsoon (in March) can be explained by the relative increase in solar radiation enhancing the photochemical aging of secondary organic aerosols over the IGP. Similar to WSOC/OC, the fractional contribution of secondary organic carbon in total OC during winter months show small variability compared to that in preceding sampling days (in March, Figure 4). The relative decrease in percentage contribution of OC_{sec} to total OC mass in late winter is due to decrease in source strength of biomass burning emissions relative to that from the fossil- fuel combustion in the upwind source regions of IGP and its subsequent long-range atmospheric to the sampling site.

3.3. Comparison of mass absorption efficiencies of WSOC and EC

The absorption of solar radiation by the EC or light absorbing WSOC can be represented by the following equation.

Absorption $\propto \lambda^{-\alpha}$; where alpha refers to angstrom exponent.

Since the mass absorption efficiency of an absorbing component is proportional to the absorption; the above equation can be rewritten as follows:

Mass absorption efficiency (MAE or σ) $\propto \lambda^{-\alpha}$

Here the mass absorption efficiency is expressed in terms of $\text{m}^2 \text{g}^{-1}$. It has been suggested that EC shows little dependency on wavelength with an angstrom exponent of around 1 (Kirchstetter *et al.*, 2004). However, significantly higher alpha (α) values were documented in the literature for particulate organic matter from biomass/bio-fuel burning emissions (Hoffer *et al.*, 2006; Kirchstetter *et al.*, 2004; Lukacs *et al.*, 2007; Hecobian *et al.*, 2010;

Cheng et al., 2011; Kirchstetter and Thatcher., 2012; Chakraborty et al., 2013; Feng et al., 2013).

For comparison, we have also estimated the MAE of EC (similar to the approach suggested by Ram and Sarin, [2009]) using Sun-set EC-OC analyzer where the attenuation of light by EC is measured at 678 nm. Since the MAE of EC is inversely proportional to wavelength (the suggested angstrom exponent value is one for EC by Kirchstetter et al., 2004), we can estimate the mass absorption efficiency of EC at other wavelengths (i.e., < 678 nm).

$$(\sigma_{EC})_{\lambda 1} \approx \lambda_1^{-1} \text{ and } (\sigma_{EC})_{\lambda 2} \approx \lambda_2^{-1}$$

In this equation, the monthly averaged MAE of EC at 678 nm has been used to estimate the σ_{EC} at other wavelengths as follows.

$$(\sigma_{EC})_{\lambda 2} = (\sigma_{EC})_{\lambda 1} * [\lambda_2/\lambda_1]^{-1}$$

Likewise, we have used the MAE of light absorbing WSOC measured at 365 nm to obtain MAE at other wavelengths

$$(\sigma_{WSOC})_{\lambda 2} = (\sigma_{WSOC})_{\lambda 1} * [\lambda_2/\lambda_1]^{-\alpha}$$

Fig.5 depicts the relative contribution of MAE of WSOC to that of EC, assessed based on monthly averaged σ_{EC} and σ_{WSOC} during the atmospheric outflow to the Bay of Bengal during November'09-March'10. From this figure, it can be inferred that the relative contribution of MAE of WSOC is maximum during the wintertime (January), compared to remaining sampling days (Fig 5), when the ratio of mass absorption efficiency of light absorbing WSOC relative to EC is ~ 0.72 . It is important to note that relatively higher contribution in early winter samples could be due to dominant contribution from agricultural crop-residue burning emissions which occur in the upwind source regions of the IGP during October-November [Rajput et al., 2014]. However, the impact of bio-fuel emissions in the IGP is more pronounced during the continental outflow to the Bay of Bengal [Kumar et al., 2010; Ram and Sarin, 2011; Ram et al., 2012; Srinivas et al., 2011; Srinivas and Sarin, 2013c]. The results reported in this study are somewhat consistent with that documented for residential bio-fuels by Kirchstetter and Thatcher, [2012]. Their study documented that the fraction of solar radiation absorbed by particulate organics generated from the bio-fuel emissions show a peak at 0.7 at 300 nm and decreased to 0.26 at 550 nm.

3.4. Implications

The measurements of optical and chemical properties of atmospheric constituents have shown the dominant nature of the anthropogenic aerosols over the Bay of Bengal compared to that over the Arabian Sea [Kedia *et al.*, 2010; Kumar *et al.*, 2008; Srinivas *et al.*, 2011; Srinivas and Sarin, 2013a; Sudheer and Sarin, 2008; Vinoj *et al.*, 2004]. In this context, atmospheric outflow from the Indo-Gangetic Plain is responsible for wide spread dispersal of pollutants over the Bay of Bengal. The atmospheric radiative forcing estimates have suggested a relative decrease in solar insolation at the surface Bay of Bengal compared to the Arabian Sea [Kedia *et al.*, 2010; Vinoj *et al.*, 2004]. Furthermore, it is suggested that aerosols over BoB are of “more absorbing” type compared to that over the ARS [Kedia *et al.*, 2010; Nair *et al.*, 2008]. Therefore, aerosol direct radiative forcing estimate increases with the absorbing BC concentration over this oceanic region. Our study demonstrates ubiquitous presence of BrC in the atmospheric outflow from the Indo-Gangetic Plain. Due to the dominance of particulate organic matter in the IGP-outflow (OC: ~ 34 % of PM_{2.5} mass; WSOC/OC: 0.52 ± 0.10) compared to EC (Av: ~ 5 %), it is, thus, important to include the absorption from brown carbon in radiative forcing estimates over the oceanic regions (BoB) located downwind of the pollution sources. Thus, presence of BrC over Bay of Bengal in addition to EC [Srinivas and Sarin, 2013a], would lead to further decrease in incoming short wave (solar) radiation and, therefore, would reduce surface radiative forcing estimates. Any changes that decrease the solar insolation can influence circulation pattern in the ocean surface. To sum-up, we suggest that the combined effect of BrC and BC needs reassessment in model estimates of aerosol radiative forcing over the Northern Indian Ocean.

The absorption of solar radiation by atmospheric water-soluble organic carbon (WSOC), relative to that by elemental carbon (EC), in the atmospheric outflow from the IGP is estimated by following the approach similar to that suggested by Kirillova *et al.* [2014]. Briefly, the absorption by WSOC is estimated as a product of the solar emission flux and the attenuation of light by WSOC (integrated over a broad wavelength range between 300 to 2500 nm) and normalized to that of EC. The wavelength dependent solar emission flux ($I_0(\lambda)$) is obtained through the clear sky Air Mass 1 Global Horizontal (AM1GH) solar irradiance model by Levinson *et al.*, [2010]. The light attenuation in the atmosphere by an absorbing species (in this case, WSOC and EC) can be estimated from the Beer-Lambert’s law (for more details, see [Kirillova *et al.*, 2014 and references therein]) as follows:

$$\frac{I_0 - I}{I_0}(\lambda, X) = 1 - e^{-\left(\sigma_X \left[\frac{\lambda_0}{\lambda}\right]^\alpha C_X h_{ABL}\right)}$$

411

412 Here σ_x and α refers to mass absorption cross section or efficiency (expressed in $\text{m}^2 \text{g}^{-1}$) and
 413 angstrom exponent, respectively, for the absorbing species X (i.e., WSOC or EC); λ_0 is 365
 414 nm for WSOC and 678 nm for EC (as explained above) whereas λ refer to any wavelength
 415 between 300 to 2500 nm. Likewise, C_x and h_{ABL} correspond to mass concentration of
 416 absorbing species (g m^{-3}) and atmospheric boundary layer height (1000 m), respectively.

417 Using this equation, we have estimated attenuation of solar radiation by WSOC and
 418 EC in the atmospheric outflow from the IGP. Furthermore, the fractional contribution of solar
 419 absorption by WSOC relative to EC is estimated as follows (adopted from Kirillova et al.,
 420 [2014]).

$$f = \frac{\int_{300}^{2500} I_0(\lambda) \left[\frac{I_0 - I}{I_0}(\lambda, WSOC) \right] d\lambda}{\int_{300}^{2500} I_0(\lambda) \left[\frac{I_0 - I}{I_0}(\lambda, EC) \right] d\lambda}$$

421

422 We have estimated the fractional contribution of solar absorption by light absorbing WSOC
 423 relative to that of EC in the atmospheric outflow from the Indo-Gangetic Plain to the Bay of
 424 Bengal. Fig. 6 depicts the fractional solar absorption of WSOC relative to that of EC in the
 425 IGP-outflow during the study period. From this figure, it is implicit to infer that the amount
 426 of solar radiation absorbed by WSOC relative to that by EC varied from 2 – 34 %.

427 Although absorption of solar radiation by WSOC (relative to EC) is estimated using
 428 a simple approach (this study), caution needs to be exercised while interpreting these results
 429 Fig. 6). It has been suggested that light absorption of OC in the solvent extracts could be
 430 underestimated by a factor of two [Liu et al., 2013]. Therefore, the estimated relative
 431 radiative forcing of light absorbing WSOC relative to EC has inherent uncertainty. However,
 432 the recent study by Kirillova et al., [2014] suggested that the warming effect caused by
 433 atmospheric brown carbon (through direct and indirect effects) could offset the net cooling
 434 effect estimated for projected WSOC concentrations. Based on radiative transfer modelling, it
 435 is suggested that brown carbon could reduce radiative forcing by ~ 20 %, at top of the
 436 atmosphere, on a global scale; thus, emphasizing this component as crucial for assessing the
 437 aerosol direct effect [Liu et al., 2014]. The significant contribution of light absorbing WSOC

in the atmospheric outflow from IGP, therefore, suggests a need for reassessment of the climate impact of this species on a global scale.

Acknowledgements

This study was supported by ISRO-Geosphere Biosphere Programme (GBP). Authors would like to thank A. Sarkar, T.K. Dalai and R. Rengarajan for extending logistic support at IIT Kharagpur. We thank the two anonymous reviewers' for their constructive comments and suggestions that helped in revising the manuscript.

References

- Agarwal, S., et al. (2010), Size distributions of dicarboxylic acids, ketoacids, alpha-dicarbonyls, sugars, WSOC, OC, EC and inorganic ions in atmospheric particles over Northern Japan: implication for long-range transport of Siberian biomass burning and East Asian polluted aerosols, *Atmos. Chem. Phys.*, 10(13), 5839-5858.
- Alexander, D. T. L., et al. (2008), Brown Carbon Spheres in East Asian Outflow and Their Optical Properties, *Science*, 321(5890), 833-836.
- Andreae, M., and A. Gelencsér (2006), Black carbon or brown carbon? The nature of light-absorbing carbonaceous aerosols, *Atmospheric Chemistry and Physics*, 6(10), 3131-3148.
- Andreae, M. O. (1983), Soot carbon and excess fine potassium: Long-range transport of combustion-derived aerosols, *Science*, 220(4602), 1148-1151.
- Andreae, M. O., et al. (1984), Long-range transport of soot carbon in the marine atmosphere, *Science of The Total Environment*, 36(0), 73-80.
- Andreae, M. O., and P. Merlet (2001), Emission of trace gases and aerosols from biomass burning, *Global Biogeochemical Cycles*, 15(4), 955-966.
- Bond, T. C. (2001), Spectral dependence of visible light absorption by carbonaceous particles emitted from coal combustion, *Geophys. Res. Lett.*, 28, 4075-4078
- Bond, T. C., et al. (2013), Bounding the role of black carbon in the climate system: A scientific assessment, *Journal of Geophysical Research: Atmospheres*, n/a-n/a.
- Bones, D. L., et al. (2010), Appearance of strong absorbers and fluorophores in limonene-O₃ secondary organic aerosol due to NH₄⁺-mediated chemical aging over long time scales, *Journal of Geophysical Research: Atmospheres*, 115(D5), D05203.
- Chakrabarty, R. K., et al. (2010), Brown carbon in tar balls from smoldering biomass combustion, *Atmos. Chem. Phys.*, 10(13), 6363-6370.
- Chakrabarty, R. K., et al. (2013), Funeral Pyres in South Asia: Brown Carbon Aerosol Emissions and Climate Impacts, *Environmental Science & Technology Letters*, 1(1), 44-48.
- Chen, Y., and T. C. Bond (2010), Light absorption by organic carbon from wood combustion, *Atmos. Chem. Phys.*, 10(4), 1773-1787.
- Cheng, Y., et al. (2011), Mass absorption efficiency of elemental carbon and water-soluble organic carbon in Beijing, China, *Atmospheric Chemistry and Physics*, 11(22), 11497-11510.

480 Draxler, R. R. (2002), HYSPLIT-4 user's guide, NOAA Tech Memo, ERL ARL-230, 35.

481 Falkovich, A., et al. (2005), Low molecular weight organic acids in aerosol particles from
 482 Rondonia, Brazil, during the biomass-burning, transition and wet periods,
 483 Atmospheric Chemistry and Physics, 5(3), 781-797.

484 Favez, O., et al. (2009), Evidence for a significant contribution of wood burning aerosols to
 485 PM_{2.5} during the winter season in Paris, France, Atmospheric Environment, 43(22-
 486 23), 3640-3644.

487 Feng, Y., et al. (2013), Brown carbon: a significant atmospheric absorber of solar radiation?,
 488 Atmospheric Chemistry and Physics, 13(17), 8607-8621.

489 Flament, P., et al. (2011), Mineral dust and carbonaceous aerosols in West Africa: Source
 490 assessment and characterization, Atmospheric Environment, 45(22), 3742-3749.

491 Forster, P., et al. (2007) (Ed.) (2007), Changes in atmospheric constituents and in radiative
 492 forcing, in Climate Change 2007: The Physical Science Basis. Contribution of
 493 Working Group I to the Fourth Assessment Report of the Intergovernmental Panel on
 494 Climate Change., 129- 234 pp., Cambridge Univ. Press, Cambridge, U. K.

495 Fuzzi, S., et al. (2006), Critical assessment of the current state of scientific knowledge,
 496 terminology, and research needs concerning the role of organic aerosols in the
 497 atmosphere, climate, and global change, Atmos. Chem. Phys., 6(7), 2017-2038.

498 Gelencser, A., et al. (2003), In-situ formation of light-absorbing organic matter in cloud water,
 499 Journal of atmospheric chemistry, 45(1), 25-33.

500 Gelencser, A., and Z. Varga (2005), Evaluation of the atmospheric significance of multiphase
 501 reactions in atmospheric secondary organic aerosol formation, Atmos. Chem. Phys, 5,
 502 2823-2831.

503 Graber, E. R., and Y. Rudich (2006), Atmospheric HULIS: How humic-like are they? A
 504 comprehensive and critical review, Atmos. Chem. Phys., 6(3), 729-753.

505 Graham, B., et al. (2002), Water-soluble organic compounds in biomass burning aerosols
 506 over Amazonia 1. Characterization by NMR and GC-MS, Journal of Geophysical
 507 Research: Atmospheres (1984-2012), 107(D20), LBA 14-11-LBA 14-16.

508 Guazzotti, S., et al. (2003), Characterization of carbonaceous aerosols outflow from India and
 509 Arabia: Biomass/biofuel burning and fossil fuel combustion, Journal of Geophysical
 510 Research: Atmospheres (1984-2012), 108(D15).

511 Gustafsson, O., et al. (2009), Brown Clouds over South Asia: Biomass or Fossil Fuel
 512 Combustion?, Science, 323(5913), 495-498.

513 Havers, N., et al. (1998), Spectroscopic characterization of humic-like substances in airborne
 514 particulate matter, *J. Atmos. Chem.*, , 29, 45-54
 515 Hecobian, A., et al. (2010), Water-Soluble Organic Aerosol material and the light-absorption
 516 characteristics of aqueous extracts measured over the Southeastern United States,
 517 *Atmos. Chem. Phys.*, 10(13), 5965-5977.
 518 Hoffer, A., et al. (2006), Optical properties of humic-like substances (HULIS) in biomass-
 519 burning aerosols, *Atmospheric Chemistry and Physics*, 6(11), 3563-3570.
 520 Huebert, B. J., and R. J. Charlson (2000), Uncertainties in data on organic aerosols, *Tellus B*,
 521 52(5), 1249-1255.
 522 Kawamura, K., et al. (2013), Determination of gaseous and particulate carbonyls
 523 (glycolaldehyde, hydroxyacetone, glyoxal, methylglyoxal, nonanal and decanal) in the
 524 atmosphere at Mt. Tai, *Atmospheric Chemistry and Physics*, 13(10), 5369-5380.
 525 Kedia, S., et al. (2010), Spatiotemporal gradients in aerosol radiative forcing and heating rate
 526 over Bay of Bengal and Arabian Sea derived on the basis of optical, physical, and
 527 chemical properties, *Journal of Geophysical Research: Atmospheres* (1984-2012),
 528 115(D7).
 529 Kirchstetter, T., and T. Thatcher (2012), Contribution of organic carbon to wood smoke
 530 particulate matter absorption of solar radiation, *Atmospheric Chemistry and Physics*,
 531 12(14), 6067-6072.
 532 Kirchstetter, T. W., et al. (2004), Evidence that the spectral dependence of light absorption by
 533 aerosols is affected by organic carbon, *Journal of Geophysical Research:*
 534 *Atmospheres*, 109(D21), D21208.
 535 Kirillova, E. N., et al. (2014), Sources and light absorption of water-soluble organic carbon
 536 aerosols in the outflow from northern China, *Atmospheric Chemistry and Physics*,
 537 14(3), 1413-1422.
 538 Kumar, A., et al. (2008), Chemical characteristics of aerosols in MABL of Bay of Bengal and
 539 Arabian Sea during spring inter-monsoon: a comparative study, *Journal of earth*
 540 *system science*, 117(1), 325-332.
 541 Kumar, A., et al. (2010), Aerosol iron solubility over Bay of Bengal: Role of anthropogenic
 542 sources and chemical processing, *Marine Chemistry*, 121(1 - 4), 167-175.
 543 Lack, D. A., et al. (2012), Brown carbon absorption linked to organic mass tracers in biomass
 544 burning particles, *Atmos. Chem. Phys.*, 13(5), 2415-2422.
 545 Levinson, R., et al. (2010), Measuring solar reflectance-Part I: Defining a metric that
 546 accurately predicts solar heat gain, *Solar Energy*, 84(9), 1717-1744.

547 Limbeck, A., et al. (2003), Secondary organic aerosol formation in the atmosphere via
 548 heterogeneous reaction of gaseous isoprene on acidic particles, *Geophysical Research*
 549 *Letters*, 30(19), 1996.

550 Liu, J., et al. (2013), Size-resolved measurements of brown carbon and estimates of their
 551 contribution to ambient fine particle light absorption based on water and methanol
 552 extracts, *Atmospheric Chemistry and Physics Discussions*, 13(7), 18233-18276.

553 Liu, J., et al. (2014), Brown Carbon in the Continental Troposphere, *Geophysical Research*
 554 *Letters*, 2013GL058976.

555 Lukacs, H., et al. (2007), Seasonal trends and possible sources of brown carbon based on
 556 2- year aerosol measurements at six sites in Europe, *Journal of Geophysical*
 557 *Research: Atmospheres* (1984-2012), 112(D23).

558 Lukács, H., et al. (2007), Seasonal trends and possible sources of brown carbon based on 2-
 559 year aerosol measurements at six sites in Europe, *Journal of Geophysical Research:*
 560 *Atmospheres*, 112(D23), D23S18.

561 Mayol-Bracero, O., et al. (2002), Carbonaceous aerosols over the Indian Ocean during the
 562 Indian Ocean Experiment (INDOEX): Chemical characterization, optical properties,
 563 and probable sources, *Journal of Geophysical Research: Atmospheres* (1984-2012),
 564 107(D19), INX2 29-21-INX22 29-21.

565 Nair, V. S., et al. (2008), Aerosol characteristics in the marine atmospheric boundary layer
 566 over the Bay of Bengal and Arabian Sea during ICARB: Spatial distribution and
 567 latitudinal and longitudinal gradients, *Journal of Geophysical Research: Atmospheres*
 568 (1984-2012), 113(D15).

569 Nguyen, T. B., et al. (2010), High-resolution mass spectrometry analysis of secondary
 570 organic aerosol generated by ozonolysis of isoprene, *Atmospheric Environment*, 44(8),
 571 1032-1042.

572 Nguyen, T. B., et al. (2012), Formation of nitrogen- and sulfur-containing light-absorbing
 573 compounds accelerated by evaporation of water from secondary organic aerosols,
 574 *Journal of Geophysical Research: Atmospheres* (1984-2012), 117(D1).

575 Nguyen, T. B., et al. (2013), Brown carbon formation from ketoaldehydes of biogenic
 576 monoterpenes, *Faraday Discussions*, 165(0), 473-494.

577 Novakov, T., et al. (2000), Origin of carbonaceous aerosols over the tropical Indian Ocean:
 578 Biomass burning or fossil fuels?, *Geophysical Research Letters*, 27(24), 4061-4064.

579 Park, R. J., et al. (2010), A contribution of brown carbon aerosol to the aerosol light
580 absorption and its radiative forcing in East Asia, *Atmospheric Environment*, 44(11),
581 1414-1421.

582 Rajput, P., et al. (2014), Characteristics and emission budget of carbonaceous species from
583 post-harvest agricultural-waste burning in source region of the Indo-Gangetic Plain,
584 *Tellus B*, 66(doi: tellusb.v66.21026).

585 Ram, K., and M. Sarin (2009), Absorption coefficient and site-specific mass absorption
586 efficiency of elemental carbon in aerosols over urban, rural, and high-altitude sites in
587 India, *Environmental Science & Technology*, 43(21), 8233-8239.

588 Ram, K., and M. Sarin (2010), Spatio-temporal variability in atmospheric abundances of EC,
589 OC and WSOC over Northern India, *Journal of Aerosol Science*, 41(1), 88-98.

590 Ram, K., et al. (2010), A 1 year record of carbonaceous aerosols from an urban site in the
591 Indo-Gangetic Plain: Characterization, sources, and temporal variability, *J. Geophys.*
592 *Res.*, 115(D24), D24313.

593 Ram, K., and M. Sarin (2011), Day-night variability of EC, OC, WSOC and inorganic ions in
594 urban environment of Indo-Gangetic Plain: implications to secondary aerosol
595 formation, *Atmospheric Environment*, 45(2), 460-468.

596 Ram, K., et al. (2012), Temporal trends in atmospheric PM_{2.5}, PM₁₀, elemental carbon,
597 organic carbon, water-soluble organic carbon, and optical properties: impact of
598 biomass burning emissions in the Indo-Gangetic Plain, *Environmental Science &*
599 *Technology*, 46(2), 686-695.

600 Rengarajan, R., et al. (2007), Carbonaceous and inorganic species in atmospheric aerosols
601 during wintertime over urban and high-altitude sites in North India, *J. Geophys. Res.*,
602 112(D21), D21307.

603 Saarikoski, S., et al. (2007), Chemical composition of aerosols during a major biomass
604 burning episode over northern Europe in spring 2006: experimental and modelling
605 assessments, *Atmospheric Environment*, 41(17), 3577-3589.

606 Saleh, R., et al. (2013), Absorptivity of brown carbon in fresh and photo-chemically aged
607 biomass-burning emissions, *Atmospheric Chemistry and Physics*, 13(15), 7683-7693.

608 Sareen, N., et al. (2010), Secondary organic material formed by methylglyoxal in aqueous
609 aerosol mimics, *Atmos. Chem. Phys.*, 10(3), 997-1016.

610 Sciare, J., et al. (2008), Long-term measurements of carbonaceous aerosols in the Eastern
611 Mediterranean: evidence of long-range transport of biomass burning, *Atmospheric*
612 *Chemistry and Physics*, 8(18), 5551-5563.

613 Srinivas, B., et al. (2011), Impact of anthropogenic sources on aerosol iron solubility over the
614 Bay of Bengal and the Arabian Sea, *Biogeochemistry*, 110(1-3), 257-268.

615 Srinivas, B., and M. Sarin (2013a), Light absorbing organic aerosols (brown carbon) over the
616 tropical Indian Ocean: impact of biomass burning emissions, *Environmental Research*
617 *Letters*, 8(4), 044042.

618 Srinivas, B., and M. M. Sarin (2013b), Carbonaceous aerosols and organic mass-to-organic
619 carbon ratio in atmospheric outflow from the Indo-Gangetic Plain, *Science of The*
620 *Total Environment*, under review.

621 Srinivas, B., and M. M. Sarin (2013c), Atmospheric deposition of N, P and Fe to the
622 Northern Indian Ocean: Implications to C- and N-fixation, *Science of The Total*
623 *Environment*, 456 - 457(0), 104-114.

624 Sudheer, A. K., and M. M. Sarin (2008), Carbonaceous aerosols in MABL of Bay of Bengal:
625 Influence of continental outflow, *Atmospheric Environment*, 42(18), 4089-4100.

626 Timonen, H., et al. (2012), Characteristics, sources and water-solubility of ambient
627 submicron organic aerosol in springtime in Helsinki, Finland, *Journal of Aerosol*
628 *Science*, 56, 61-77.

629 Updyke, K. M., et al. (2012), Formation of brown carbon via reactions of ammonia with
630 secondary organic aerosols from biogenic and anthropogenic precursors, *Atmospheric*
631 *Environment*, 63(0), 22-31.

632 Vinoj, V., et al. (2004), Radiative forcing by aerosols over the Bay of Bengal region derived
633 from shipborne, island-based, and satellite (Moderate-Resolution Imaging
634 Spectroradiometer) observations, *Journal of Geophysical Research: Atmospheres*
635 (1984-2012), 109(D5).

636 Wang, H., et al. (2005), Carbonaceous and ionic components in wintertime atmospheric
637 aerosols from two New Zealand cities: Implications for solid fuel combustion,
638 *Atmospheric Environment*, 39(32), 5865-5875.

639 Yang, M., et al. (2009), Attribution of aerosol light absorption to black carbon, brown carbon,
640 and dust in China – interpretations of atmospheric measurements during EAST-
641 AIRE, *Atmos. Chem. Phys.*, 9(6), 2035-2050.

642 Zhang, X., et al. (2011), Light-absorbing soluble organic aerosol in Los Angeles and Atlanta:
643 A contrast in secondary organic aerosol, *Geophysical Research Letters*, 38(21),
644 L21810.

645 Zhang, X., et al. (2013), Sources, Composition and Absorption Angstrom Exponent of Light-
646 absorbing Organic Components in Aerosol Extracts from the Los Angeles Basin,
647 Environmental Science & Technology, 47(8), 3685-3693.
648
649
650

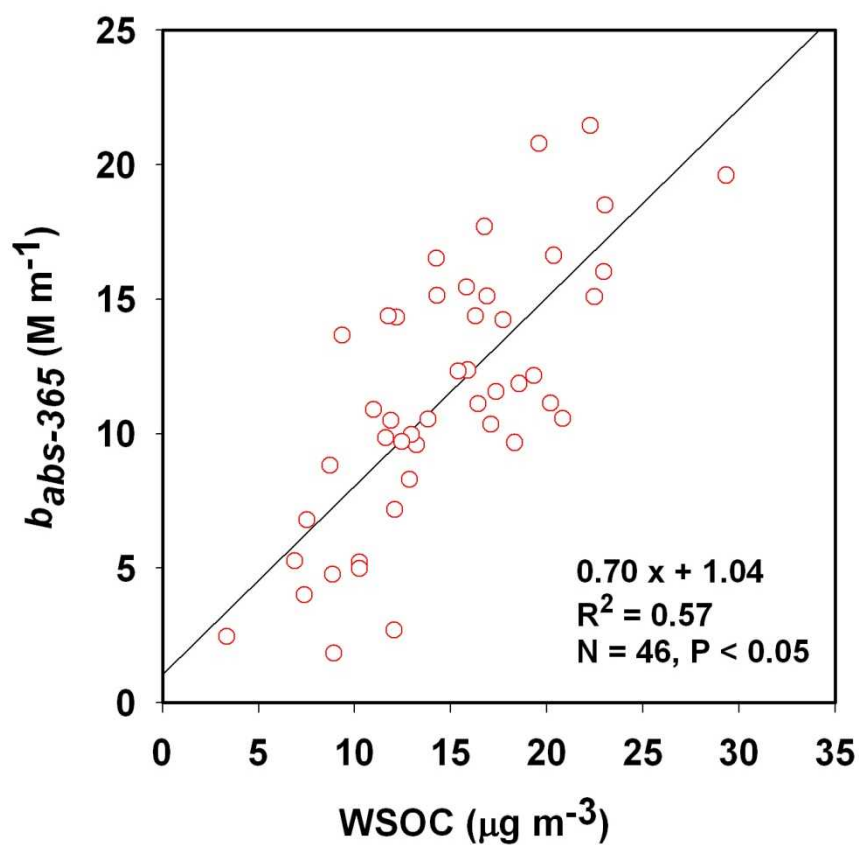


Fig.1. Scatter plot for mass concentration of water-soluble organic carbon (WSOC) and absorption coefficient (b_{abs}) at 365 nm (where $M = x \cdot 10^{-6}$).

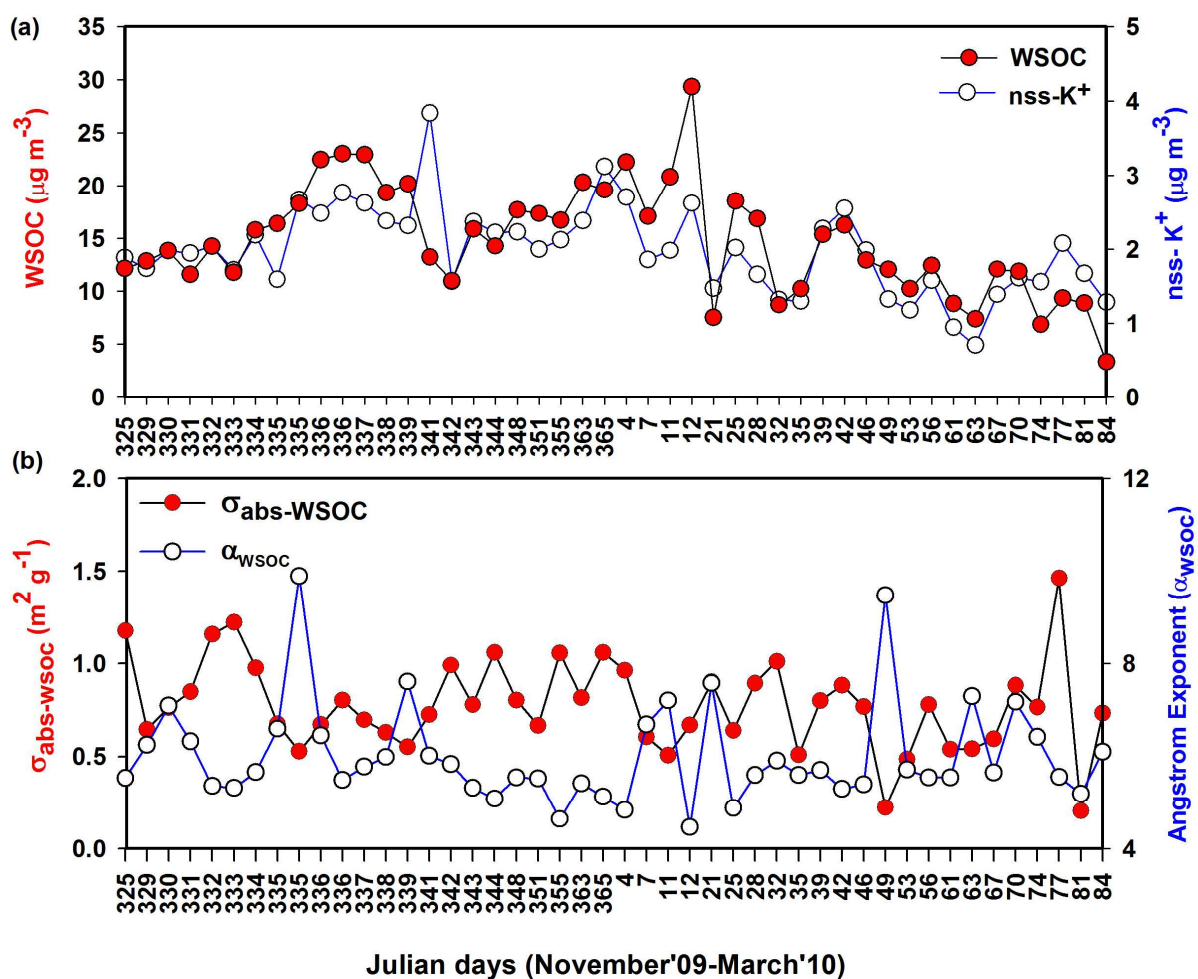
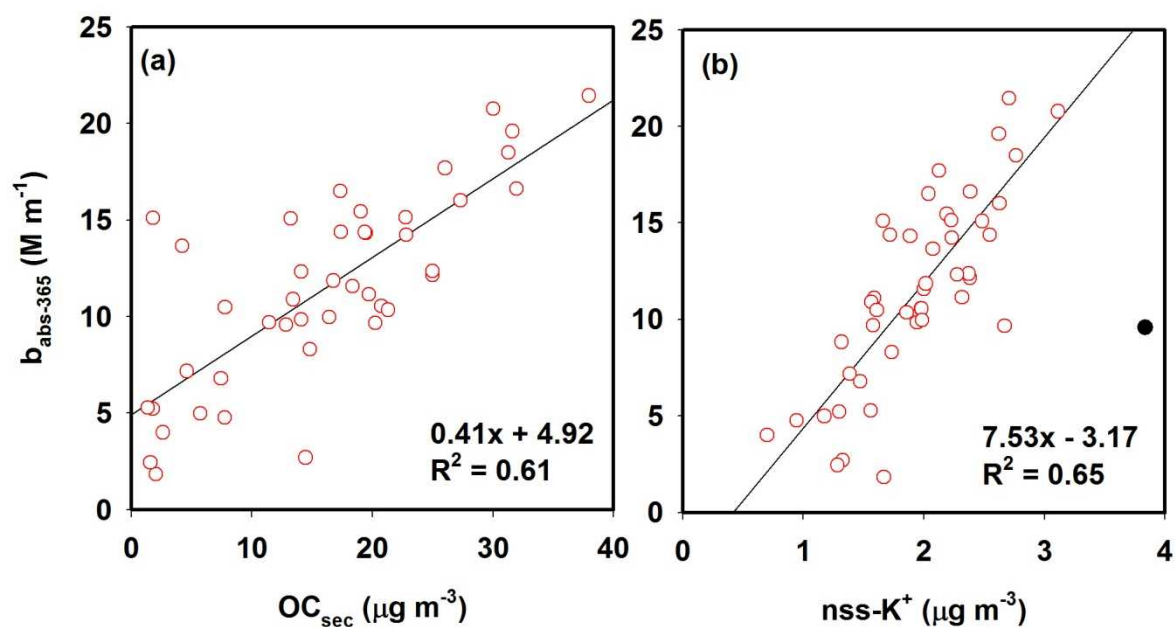


Fig.2. (a) Temporal variability of WSOC and nss- K^+ concentrations suggest their common source from biomass burning emissions, (b) temporal variability of mass absorption efficiency of light absorbing water-soluble organic carbon ($\sigma_{\text{abs-WSOC}}$) and the Angstrom exponent (α_{WSOC}) .

679
680
681



682
683
684
685
686
687

Fig. 3. A strong positive relationship of mass absorption coefficient of water-soluble organic (brown) carbon with the abundance of secondary organic carbon (OC_{sec}) and nss-K^+ , suggests the formation of atmospheric brown carbon from biogenic secondary organic aerosols over the IGP.

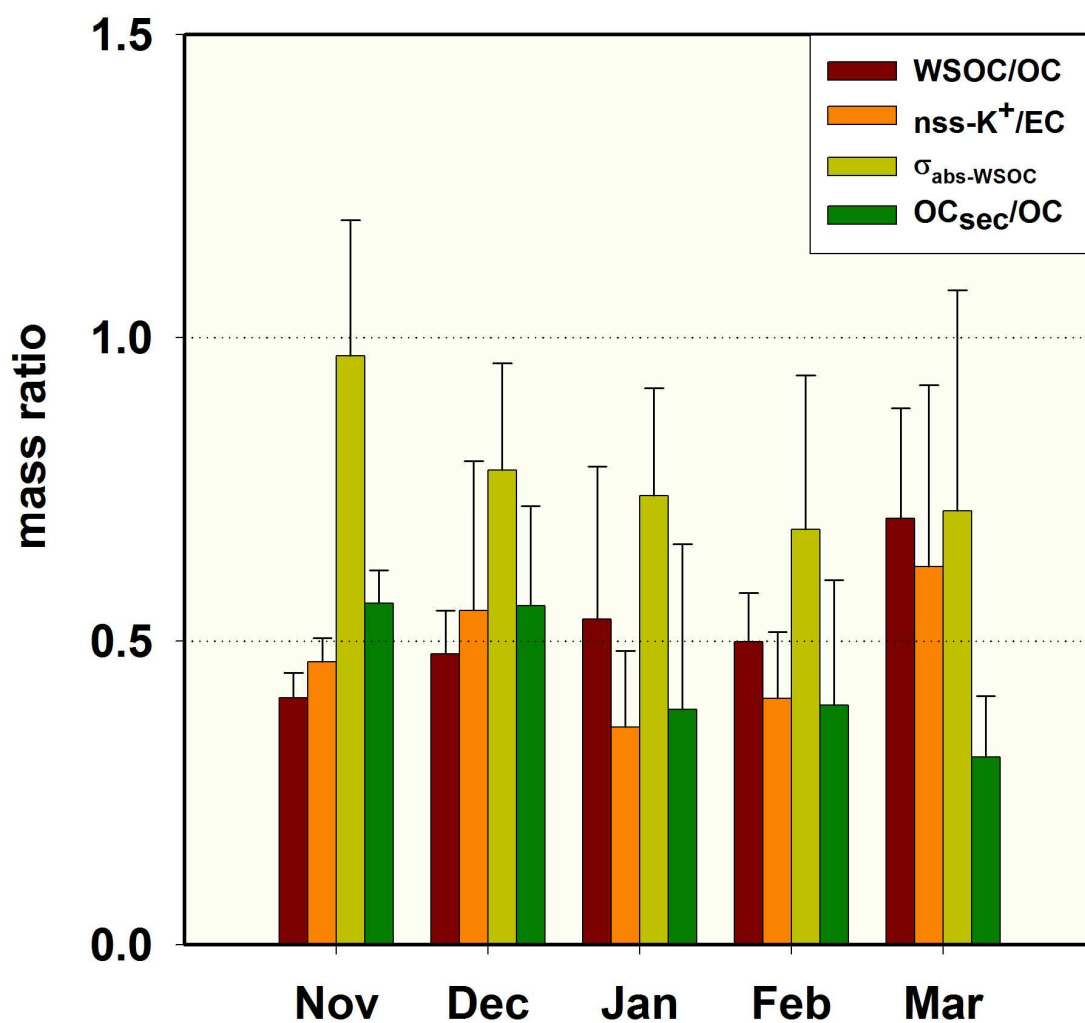


Fig.4. Temporal variability of diagnostic mass ratios (WSOC/OC, nss-K⁺/EC, OC_{sec}/OC) and mass absorption efficiency of light absorbing brown carbon (σ_{abs}-WSOC).

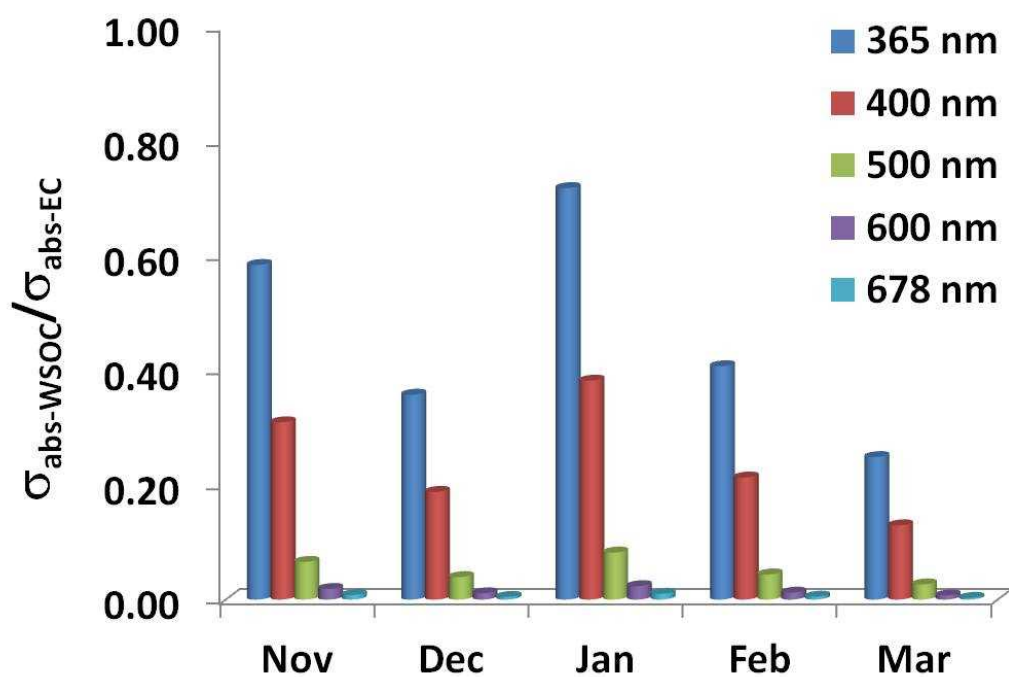


Fig.5. Fractional contribution of mass absorption efficiency of light absorbing water-soluble organic carbon (WSOC) to that of elemental carbon (EC) in the atmospheric outflow to the Bay of Bengal during November'09 – March'10.

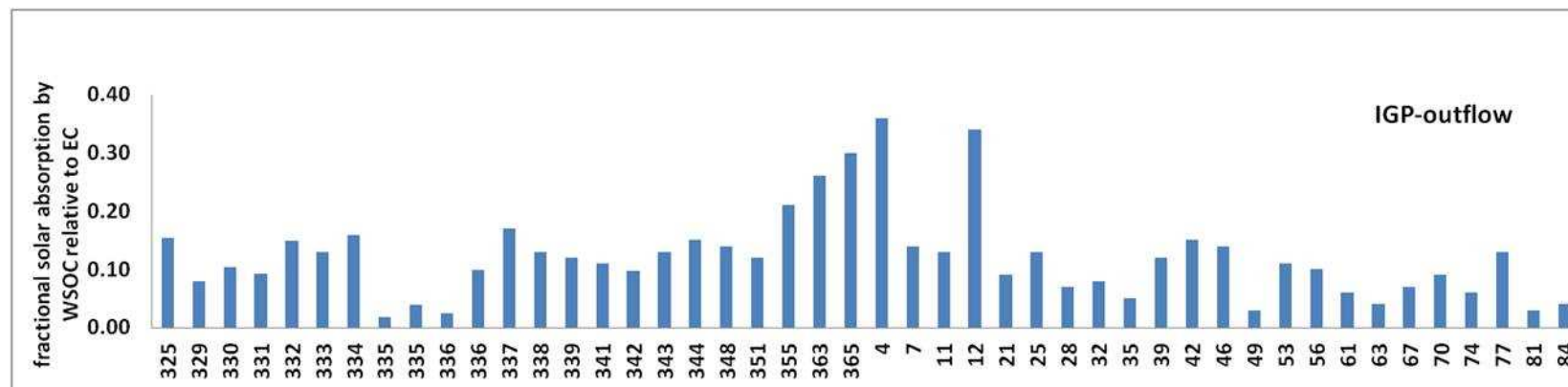


Fig.6. Solar absorption by WSOC relative to EC in the atmospheric outflow from the Indo-Gangetic Plain to the Bay of Bengal during November'09 – March'10.

Table 1. Comparison of mass absorption efficiency (σ_{abs}) and angstrom exponent (\AA_p) of brown carbon (BrC) in the atmospheric outflow from the Indo-Gangetic Plain with other literature studies.

Region	Source	$\lambda(\text{nm})$	$\sigma_{\text{abs-BrC}} (\text{m}^2 \text{g}^{-1})$	α_{wsoc}	Reference
Indo-Gangetic Plain	BB/BF-E	365	0.78 ± 0.24	6.0 ± 1.1	This study
Bay of Bengal (IGP-outflow)	BB/BF-E	365	0.4 ± 0.1	9.1 ± 2.5	Srinivas and Sarin, 2013a
Bay of Bengal (SEA-outflow)	BB/BF-E	365	0.5 ± 0.2	6.9 ± 1.9	Srinivas and Sarin, 2013a
Los-Angeles, USA	BBE	365	0.71	7.6 ± 0.5	Zhang et al., 2013
North America	BBE	404	0.82 ± 0.43	-	Lack et al., 2012
Beijing, China	BBE	550	0.5	-	Yang et al., 2009
Beijing, China	BBE	365	1.8 ± 0.2 (summer)	7.5 ± 0.9	Cheng et al., 2011
Beijing, China	BBE	365	0.7 ± 0.2 (Winter)	7.0 ± 0.8	Cheng et al., 2011
South-eastern US & Atlanta, Georgia	BBE	365	0.64 (urban) & 0.58 (rural)	7 ± 1	Hecobian et al., 2010
Amazon basin	BBE	350 - 400	$\sim 0.5 - 1.5$	$\sim 6 - 7$	Hoffer et al., 2006